Design of Magneto-Rheological Fluid Based Device

Jeong-Hoon Kim, Chong-Won Lee*, Byung-Bo Jung, Youngjin Park
Center for Noise & Vibration Control, Department of Mechanical Engineering, KAIST, Taejon 305-701, Korea
Guangzhong Cao
School of Engineering and Technology, Shenzhen University, Shenzhen, Guangdong, 518060, P.R.China

The effect of power supply voltage on the performance limits in a laboratory magneto-rheological fluid based device was identified by experiments. It suggests that the frequency range of motion for control is limited by the voltage attenuation due to the coil inductance and the maximum power supply voltage set for practical use of an MRF devices. In this work, the magnetic and electrical characteristics of the MRF device are investigated and a design procedure is formulated to achieve the desired performance for a given power supply.

Key Words : Magneto-Rheological Fluid, Yield Stress, Slew Rate, Power Supply Voltage, Design Procedure

1. Introduction

Magneto-rheological fluid(MRF) changes its rheological characteristics according to the applied magnetic field strength. The fluid typically consists of micron-size, magnetically polarizable particles dispersed in a carrier medium. The formation of particle chains upon the application of a magnetic field is essential to operation of MRF(Weiss et al., 1993). In the presence of shear force, the equilibrium that is established between the formation and breaking of particle fabrics corresponds to the yield stress defined for the fluid. The controllable control force of an MRF device makes use of the yield stress. This simple and easy change of its characteristics without mechanical moving parts makes it possible to provide simple, quiet, rapid-response electromechanical devices(Carlson et al., 1994 and 1996). Thus MRF devices have attracted much attention among control and design engineers in the past decade and are considered as a technical breakthrough for 'smart' electromechanical devices, especially stress transfer and damping devices(Rankin et al., 1998). Not only their feasibility is being widely demonstrated, but also their many advantages against the conventional passive and fully active engineering devices are becoming apparent. On the other hand, it is also important to recognize and understand the shortcomings of MRF devices (Kim et al. 1996). Among others, two major problems occur frequently in the engineering applications of MRF. The rate at which the yield stress of MRF can change is strictly limited due to the presence of the inductance of an MRF device and the fixed power supply voltage. This phenomenon is referred to as the yield stress slew rate limitation. The maximum yield stress is also subject to a strict limit due to the magnetic saturation and the fixed power supply voltage.

It has been widely known that an advantage of MRF devices is the utilization of low voltage, current driven power supply, unlike electro-rheological fluid which requires high voltage power supply for implementation of controllable devices(Ahn et al., 1998, Carlson et al., 1996,

* Corresponding Author,
E-mail : cwlee@novic.kaist.ac.kr
TEL : +82-42-869-3016; **FAX** : +82-42-869-8220
Center for Noise & Vibration Control, Department of Mechanical Engineering, KAIST, Taejon 305-701, Korea. (Manuscript **Received** April 16, 2001; **Revised** July 31, 2001)

Choi and Choi, 1999 and Weiss et al., 1993). MRF devices are designed to guarantee the desired maximum yield stress by avoiding the magnetic saturation and using the power supply voltage just greater than the resistance multiplied by the maximum current (Lord Material Division, November and December 1999). In other words, power supply is not considered explicitly in the design process of an MRF device, which turns out to be inadequate to control high frequency motion. The voltage attenuation due to the coil inductance significantly increases over the high frequency range of interest. In order for the high frequency performance of the controlled motion to be enhanced, high power supply voltage is needed, since power supply voltage is one of the factors which determine the bandwidth of the MRF device. But the voltage level of power supply for the MRF device is, in practice, limited mainly due to cost, and thus power supply voltage is predetermined in the design process of the MRF device.

2. Motivation

In order to investigate the effect of the power supply voltage on the performance of an MRF device, a rotary MRF damper developed in the laboratory (Jung and Park, 1998 and 1999) for electronically controlled power steering, as shown in Fig. 1, is considered. Since the yield stress of MRF in the device is difficult to be directly measured, the control current delivered to the device was observed instead during the experiments, since the yield stress of MRF can be estimated from the measured control current. For the experiments, a uni-directional current amplifier with gain of 1 A/V was manufactured in the laboratory. For comparison, two loads were applied for two types of control commands: 7.6 ohm and 3.73 mH @ 120 Hz for load #1 and 5.1 ohm and 7.81 mH @ 120Hz for load #2. The sinusoidal and step control commands of 100 Hz to the uni-directional current amplifier were given, respectively, by

$$V_C = I = 0.5 + 0.5 \sin(200\pi t), \quad (1)$$

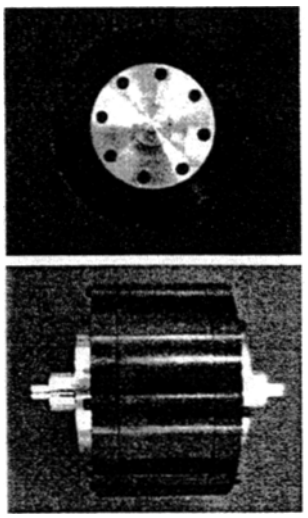

Fig. 1 Rotary MR damper for electronically controlled power steering [Jung and Park, 1998 and 1999]

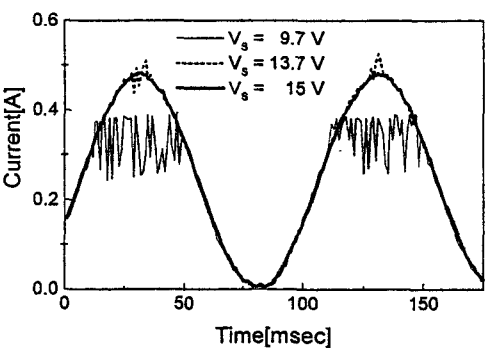

Fig. 2 Control current to sinusoidal control voltage in load 1

$$V_C = I = 1, \text{ if } \sin(200\pi t) > 0, \text{ else } V_C = I = 0. \quad (2)$$

where V_C is the control input voltage. Figures 2 and 3 show the control currents delivered to load #1 and #2, respectively, for the sinusoidal control command. For load #1, the current followed the control voltage well when the power supply voltage of 15 V was applied. But for load # 2, the desired power supply voltage dropped to 13.7 V. Note that since load #2 has a resistance smaller than load #1, the desired maximum current amplitude can be achieved with a lower power supply voltage than load #1. In this case, the resistance of a device determines the necessary

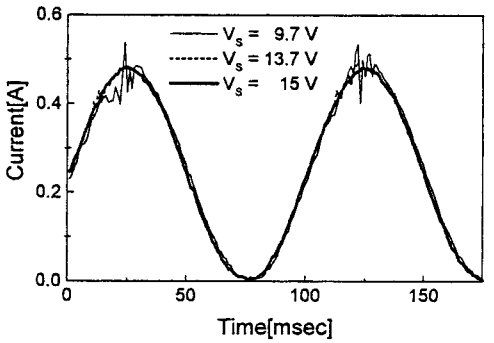

Fig. 3 Control current to sinusoidal control voltage in load 2

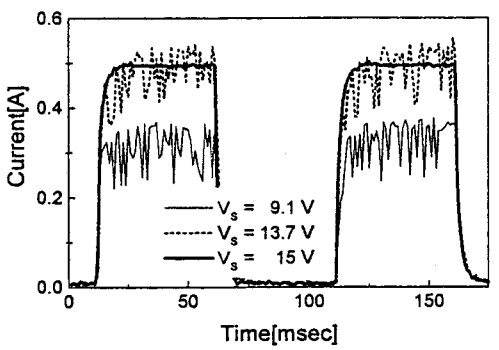

Fig. 4 Control current to step control voltage in load 1

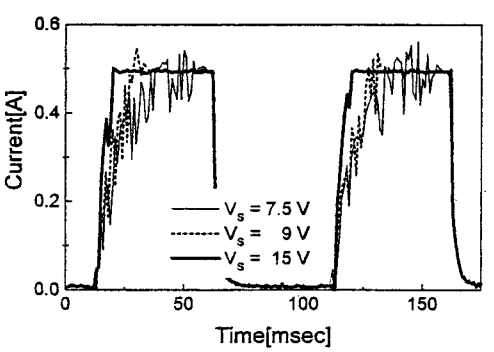

Fig. 5 Control current to step control voltage in load 2

power supply voltage. On the other hand, for the step control command having higher frequency components than the sinusoidal control command, load #2 of a higher inductance requires a higher power supply voltage to follow the control current for the step control command as shown in Figs. 4 and 5. The control current in load #2 cannot rise as fast as that in load #1. Thus the desired bandwidth of the current should be increased to follow the control command, requiring power supply voltage higher than about 15 volts. In this case, the inductance of a device determines the necessary power supply voltage. In other words, as the load becomes severer, larger power supply voltage is needed.

In practice, we often increase the number of coil turns in order to reduce the necessary maximum control current, which increases the inductance of the MRF device. This, in turn, increases the necessary power supply voltage as the frequency range of interest increases. Thus, the mechanisms which limit the performance of the MRF device should be investigated in order to predict the performance limits with a given power supply and to formulate a design procedure to achieve the desired performance of the device as a whole, which will be discussed in the following sections.

3. Governing Equations of MRF Device

3.1 Mechanical dynamic model

The dynamic behavior of MRF is often modeled as the Bingham plastic model given by (Rankin et al., 1998)

$$\tau=\tau_y sign(\dot{\gamma})+\eta_p\dot{\gamma}, \quad for\ |\tau|\geq|\tau_y| \qquad (3)$$
$$\dot{\gamma}=0, \quad for\ |\tau|<|\tau_y|$$

where τ is the shear stress; τ_y is the dynamic yield stress which is an increasing function of the magnetic field strength H; η_p is the plastic viscosity and $\dot{\gamma}$ is the shear rate. Apparent viscosity, $\eta_a \equiv \tau/\dot{\gamma}$, increases as the applied magnetic field strength and thus τ_y increases. The expression of τ_y in exponential form is usually used in the design process as

$$\tau_y=\alpha H^{\beta} \qquad (4)$$

where α is the proportionality coefficient determined from experiment and β is the exponent conventionally known as similar to 2. Two basic operational modes used for MRF devices are the

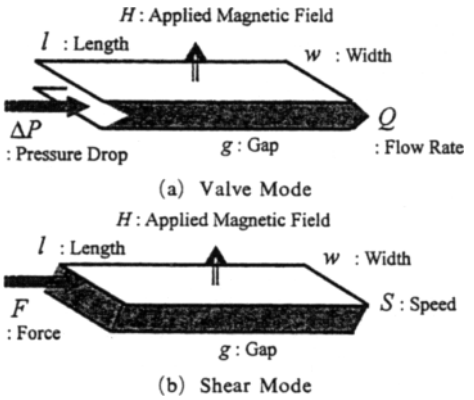

Fig. 6 Basic operational modes [Carlson et al., 1996]

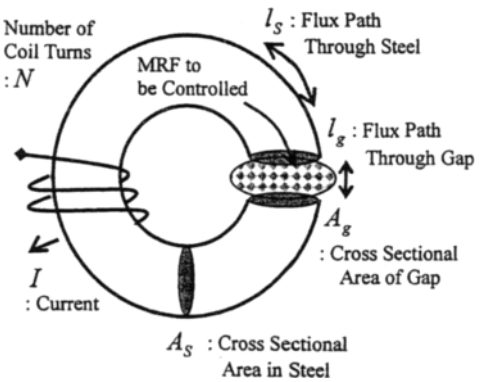

Fig. 7 Magnetic circuit of MRF device [Weiss et al., 1993]

valve and shear modes, as shown in Fig. 6. Design equations for a device utilizing either the valve or shear mode are derived using Eq. (3) (Carlson et al., 1996 and Weiss et al., 1993). The pressure drop, ΔP, in valve mode is obtained as (Duclos, 1988 and Lord Material Division, 1999b)

$$\Delta P=\frac{12\eta_p l}{g^3 w}Q+\frac{Cl}{g}\tau_y \tag{5}$$

where l and w are the length and width of the pole, respectively; g is the gap between the two poles; Q is the volume flow rate; C is the experimentally determined constant parameter ranging from a minimum value of 2 to a maximum value of 3. The resisting force, F, in shear mode is also obtained as (Duclos, 1988 and Lord Material Division, 1999b)

$$F=\frac{lw\eta_p}{g}S+lw\tau_y \tag{6}$$

where S is the relative speed of a pole to another.

Note that, as Eqs. (5) and (6) indicate, the controllable force, pressure drop ΔP or resisting force F, of the MRF device is proportional to the yield stress of MRF. The desired maximum yield stress, τ_y^*, and the plastic viscosity, η_p, govern the volume of MRF necessary to achieve the required controllable force (Carlson et al., 1996 and Weiss et al., 1993).

3.2 Magnetic circuit

A simple magnetic circuit can provide the field strength needed to activate and control MRF as shown in Fig. 7. The basic relations with the assumption of no magnetic saturation become (Carlson et al., 1994 and Lord Material Division, 1999a)

$$B_S A_S=B_g A_g \tag{7}$$

$$H_S l_S(\approx 0)+H_g l_g=NI \tag{8}$$

where B is the flux density; l is the flux path length; A is the cross sectional area; I is the current; N is the number of coil turns. The subscripts S and g denote the steel and gap, respectively. The flux path length and cross sectional area of gap determine the amount of steel required to achieve the desired field strength and yet to avoid magnetic saturation as in Eq. (7). The flux path length in MRF, l_g, is a linear function of the gap, g, whose concrete form is determined according to the application. The reluctance of steel is much less than that of MRF and thus it can be neglected in the design process as in Eq. (8).

The most immediately apparent limiting behavior of MRF devices is the maximum controllable force limitation, or equivalently, the maximum yield stress limitation. This limitation is primarily due to saturation in magnetization of electromagnet core materials. Eq. (8) is based on the assumption that core magnetic flux is nearly proportional to magneto motive force (MMF : coil turns×coil current). This relationship is valid as long as the magnetic reluctance of the core is much less than that of MRF in the gap. In a typical magnetic induction vs. magnetic field

curve for conventional magnet iron, the reluctance is inversely proportional to the slope of the curve. A significant feature is the leveling of the curve at high MMF's; beyond a certain point, the reluctance increases drastically. This phenomenon is referred to as magnetic saturation and the flux density at which it occurs is called the saturation flux density, which typically ranges between 1.2 and 1.6 Tesla. The effect of magnetic saturation is that, once a certain coil current is reached, further increases in current will produce relatively little increase in the yield stress of MRF (Maslen et al., 1989). Thus, in a conventional design process, the maximum yield stress of an MRF, or the maximum controllable force of MRF device, is developed at the magnetic saturation of steel, i. e.,

$$B_{sat}A_S=\mu_{MRF}\frac{A_g}{l_g}NI^* \tag{9}$$

where $B_g=\mu_{MRF}H_g$; I^* is the maximum available current in current amplifier; B_{sat} is the saturation flux density of steel; and μ_{MRF} is the magnetic permeability of MRF. So far, magnetic circuit design was carried out using Eq. (9) merely to maintain sufficient cross section of steel so that magnetic saturation can be avoided. From Eqs. (4) and (9), we can conclude that the maximum yield stress of the MRF device is limited by the maximum current of the power supply for other design variables given.

3.3 Electric circuit

The electric circuit is designed to guarantee both the adequate bandwidth for effective control of MRF devices and the desired current. The output stage of the current amplifier which drives the coil is described in Fig. 8(Maslen et al., 1989), i. e.,

$$V_S=(R+R_V+R_F)I+L\frac{dI}{dt}+V_0 \tag{10}$$

where R and L are the electrical coil resistance and inductance of solenoid which induces magnetic field in MRF, respectively; R_V is the variable resistance between the coil and ground, which varies between about 0.5 and nearly infinite ohms and is a function of V_C ; R_F is the current sensing resistance; V_S is the power supply voltage; V_0 is the additional voltage of about 5 to 6 volts required for compensation of the voltage drop which can take place in the electric circuit depending upon the type of the current amplifier.

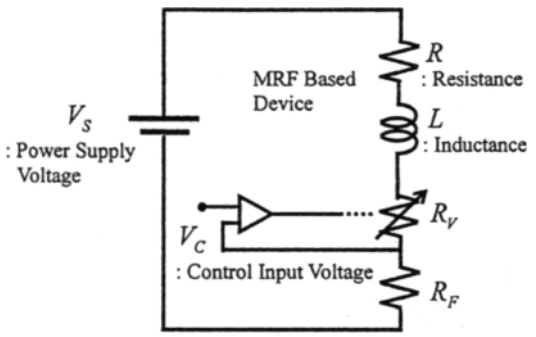

Fig. 8 Electric circuit of MRF device with current amplifier [Maslen et al., 1989]

The yield stress slew rate of MRF is limited because the magnet coil is inductive and the power supply voltage to drive the current amplifier is finite. The slew rate limitation causes the controllable force of an MRF device to lag the control signal demands, introducing a phase lag. To reduce the phase lag or to guarantee an adequate bandwidth of the MRF device for control, there should be a lower limit for power supply voltage(Maslen et al., 1989).

Until now, we investigated three models which govern behaviors of an MRF device and found the mechanisms which give rise to the yield stress and slew rate limitations. So, in the following discussion, a design procedure will be established in order to achieve the desired maximum yield stress and the desired maximum slew rate for the predetermined power supply voltage. This is essential for the practical MRF device, because, in practice, maximum available power supply voltage is predetermined and it is hard to increase the voltage optionally.

4. Design Procedure

4.1 Magnetic circuit design

It will prove convenient to assume that, in the design process, τ_y^* is given instead of the desired

maximum controllable force. In addition, it is natural to assume that the values of τ_y^*, $\left[\frac{d\tau_y}{dt}\right]^*$, α, β, B_{sat}, μ_{MRF}, μ_{Steel}, R_V^*, R_F, V_0, I^* and V_S^* are known a priori. Here, $\left[\frac{d\tau_y}{dt}\right]^*$ is the desired maximum yield stress slew rate; R_V^* is the minimum value of R_V; and V_V^* is the maximum power supply voltage. Then the design variables of the magnetic circuit become l_g, A_S, A_g and N. From Eqs. (4) and (9), we can easily obtain

$$\tau_y|_{\max}=\alpha\left[\frac{NI^*}{l_g}\right]^\beta=\alpha\left[\frac{B_{sat}}{\mu_{MRF}}\frac{A_S}{A_g}\right]^\beta\geq\tau_y^* \quad (11)$$

where $\tau_y|_{\max}$ is the maximum available yield stress in an MRF device. Eq. (11) means that it is important to maintain the sufficiently large cross section of steel in order to keep the magnetic field strength as desired. On the other hand, from Eqs. (9) and (11), we can easily obtain

$$\frac{N}{l_g}\frac{A_g}{A_S}\geq\frac{B_{sat}}{\mu_{MRF}}\frac{1}{I^*} \quad (12)$$

and

$$\frac{N}{l_g}\geq\frac{1}{I^*}\left[\frac{\tau_y^*}{\alpha}\right]^{\frac{1}{\beta}} \quad (13)$$

4.2 Electric circuit design

From Eqs. (4) and (8), the desired current slew rate can be obtained as

$$\left.\frac{d\tau_y}{dt}\right|_{\max}=\alpha\beta\left[\frac{NI^*}{l_g}\right]^{\beta-1}\frac{dI}{dt}\geq\left[\frac{d\tau_y}{dt}\right]^* \quad (14)$$

where $\left.\frac{d\tau_y}{dt}\right|_{\max}$ is the maximum available yield stress slew rate in the MRF device.

Substituting Eq. (15) into Eq. (10),

$$\frac{dI}{dt}\geq\frac{NI^*}{l_g\beta\tau_y^*}\left[\frac{d\tau_y}{dt}\right]^* \quad (15)$$

we obtain

$$V_S^*\geq(R+R_V^*+R_F)I^*+L\frac{NI^*}{l_g\beta\tau_y^*}\left[\frac{d\tau_y}{dt}\right]^* \quad (16)$$

It is generally accepted that the electrical coil resistance and inductance, R and L, are proportional to the number of coil turns, N, and the square of the number of coil turns, N^2, respectively, i. e.,

$$R=k_RN \quad (17)$$

$$L=k_LN^2 \quad (18)$$

where k_R and k_L are constants depending on the coil properties and the solenoid dimensions. Substituting Eqs. (17) and (18) into Eq. (16), we obtain

$$\frac{k_LI^*}{l_g\beta\tau_y^*}\left[\frac{d\tau_y}{dt}\right]^*N^3+k_RI^*N+(R_V^*+R_F)I^*-V_S^*\leq0 \quad (19)$$

which offers a guideline for selection of the solenoid coils and determination of the solenoid dimensions. The allowable range of N then reduces to

$$0<N\leq\sqrt[3]{\frac{-q+\sqrt{q^2+4p^3}}{2}}+\sqrt[3]{\frac{-q-\sqrt{q^2+4p^3}}{2}} \quad (20)$$

where $q=\frac{l_g\beta\tau_y^*}{k_LI^*\left[\frac{d\tau_y}{dt}\right]^*}((R_V^*+R_F)I^*-V_S^*)$ and $p=\frac{l_g\beta\tau_y^*}{3\left[\frac{d\tau_y}{dt}\right]^*}\frac{k_R}{k_L}$

4.3 Typical design procedure

Based on the previous analysis of the magnetic and electric circuits, we suggest the following typical design procedure:

1. Determine the number of coil turns, N, from Eq. (20).

2. Determine the flux path length in MRF, l_g, from Eq. (13).

3. Select the area ratio of $\frac{A_g}{A_S}$ from Eq. (12).

4. The cross sectional area of gap, $A_g=l\cdot w$, can then be determined, considering the desired controllable force, e. g., the pressure drop ΔP in Eq. (5) or the resisting force F in Eq. (6).

5. Conclusions

The mechanisms which give rise to the yield stress and slew rate limitations have been explored in some detail considering the magnetic and electric circuits of an MRF device. It was found that the yield stress limitation is due to the magnetic saturation and finite power supply voltage, and the slew rate limitation is due to the magnet coil inductance and finite power supply voltage. From the theoretical developments, the

theoretical upper bound of the number of coil turns is obtained. And finally, a design procedure was formulated to achieve the desired maximum yield stress and the desired maximum yield stress slew rate for the predetermined power supply voltage.

A rigorous verification of the theoretical developments needs extensive experiments, including identification of the unknown and nonlinear behaviors of MRF, is beyond the scope of this work and is left as a future work.

Acknowledgment

This work was supported by the Korea Science and Engineering Foundation under Contract 97-0102-03-01-3. This financial support is gratefully acknowledged.

References

Ahn, Y. K., Morishita, S. and Yang, B. S., 1998, "Directionally Controllable Squeeze Film Damper Using Liquid Crystal," KSME International Journal, Vol. 12, No. 6, pp. 1097~1103.

Carlson, J. D., Chrzan, M. J. and James, F. O., 1994, "Magnetorheological Fluid Devices," U. S. Patent # 5284330.

Carlson, J. D., Catanzarite, D. M. and St. Clair, K. A., 1996, "Commercial Magneto-Rheological Fluid Devices," Proceedings of 5th International Conference on Electro-Rheological Fluids, Magneto-Rheological Suspensions and Associated Technology. pp. 20~28.

Choi, S. B. and Choi, Y. T., 1999, "Sliding Mode Control of a Shear-Mode Type ER Engine Mount," KSME International Journal, Vol. 13, No. 1, pp. 26~33.

Duclos, T. G., 1988, "Design of Devices Using Electrorheological Fluids," Society of Automotive Engineers, SAE Paper #881134.

Jung, B. B. and Park, Y., 1998, "Electronically Controlled Power Steering by Magneto-Pheological Fluid," Proceedings of the 13th Korea Automatic Control Conference, pp. 1173~1176.

Jung, B. B. and Park, Y., 1999, "Development of Damper for Electronically Controlled Power Steering by Magneto-Rheological Fluid," Proceedings of the KSAE Spring Conference, pp. 587~591.

Kim, J. H., Lee, C. W. and Lee, S. K., 1996, "Modelling of Magneto-rheological Fluid Based Semi-active Mount," Proceedings of 3rd International Conference on Motion and Vibration Control, Vol. 3, pp. 164~169.

Lord Materials Division, November 1999, "Magnetic Circuit Design," Engineering Note.

Lord Materials Division, December 1999, "Designing with MR Fluids," Engineering Note.

Maslen, E., Hermann, P., Scott, M. and Humphris, R. R., 1989, "Practical Limits to the Performance of Magnetic Bearings : Peak Force, Slew Rate, and Displacement Sensitivity," Transactions of ASME, Journal of Tribology, Vol. 111, pp. 331~336.

Rankin, P. J., Ginder, J. M. and Klingenberg, D. J., 1998, "Electro- and Magneto-rheology," Current Opinion in Colloid & Interface Science, Vol. 3, pp. 373~381.

Weiss, K. D., Duclos, T. G., Carlson, J. D., Chrzan, M. J. and Margida, A. J., 1993, "High Strength Magneto- and Electro-rheological Fluid," SAE Paper #932451.